Granulite Microfabrics and Deformation Mechanism of Mogok Area in Myanmar

Wai Yan Lai Aung* and Day Wa Aung
Department of Geology, University of Yangon

Abstract

The Mogok Metamorphic Belt (MMB) in central Myanmar is an upper amphibolite to granulite facies terrain that is mainly composed of high-grade metamorphic rock and younger igneous intrusions. In the Mogok area, rock units are composed mainly of marbles, calc-silicate rocks, gneisses and granulites intruded by granitic and syenitic rocks. Granulites and granulitic gneisses are the oldest units of the research area. In the research, the microfabrics and deformation textures found in granulite are evaluated for the high-temperature/ultrahigh-temperature metamorphism of the Mogok area in Myanmar. The present research mainly aims to deal with the study of granulite microfabrics and the deformation mechanism significantly found in MMB. Methods of the investigations were fixed in detail based on literature reviews, field studies, petrological microscopes, and advanced techniques such as EDXRF, WDXRF, RAMAN, and EPMA analyses. The geochemistry shows that felsic granulite has a higher potassium percentage while mafic granulite yields higher calcium content. By using mineral chemistry, ultrahigh-temperature (UHT; T_{max}≥900°C) diagnostic equilibrium mineral assemblages found in granulites such as sapphirine + quartz + orthopyroxene, and orthopyroxene + sillimanite + quartz were recorded. However, the post-peak cooling-dominated and decompression-dominated reaction textures of felsic granulites are corona and symplectic textures of cordierite and spinel, while orthopyroxene-plagioclase symplectite in mafic granulite that express retrograde metamorphic *P-T* conditions estimated within the range of 6.5 ~ 7.2 kbar, 700 ~ 780°C.

Keywords: felsic and mafic granulites, microfabrics, cooling dominated, decompression dominated

1. Introduction

The research area, Mogok, is situated in the Mogok Metamorphic Belt (MMB). Mogok Valley in northern Myanmar contains some of the world's best quality ruby and other gemstones (Hughes, 1997; Iyer, 1953; Themelis, 2008) extracted from upper amphibolite to granulite facies marbles in the MMB (Chhibber, 1934a, 1934b; La Touche, 1913; Myanmar Geosciences Society, 2014; Searle & Haq, 1964; Searle *et al.*, 2007, 2017, 2020). The granulites are metamorphic rocks of the Precambrian age (Chhibber, 1934a, Searle *et. al.*, 2016), which have been rarely preserved in their original mutual contact relationships with neighboring rock masses. Mostly, they have been tectonically squeezed into alien environments. Granulites and granulite facies metamorphic rocks are formed under the most intense temperature-pressure conditions usually found in regional metamorphism (Eskola, 1952; Fyfe, Turner, and Verhoogen, 1961; Winkler, 1965). Mineral assemblages and thermobarometry indicate granulite assemblages equilibrate over a broad range of temperatures generally from about 650 to 900 °C but to as much as 1050 °C and pressures of generally 5 kbar to as much as 12 kbar, or depths of 20-45 (Harley, 1998). Ultrahigh temperature (UHT) metamorphism is a division of granulite facies metamorphism and it represents extreme crustal metamorphism with peak metamorphic temperatures exceeding 900 °C (Jiao *et. al.*, 2023) and over 1000 °C (Lei and Xu, 2018) and medium pressures ranging from 7 to 13 kbar at crustal depths of 15-55 km with or without partial melting of crusts, which is usually identified in the granulite-facies rocks (Jiao *et. al.*, 2023, Lei and Xu, 2018). There are approximately 110 localities worldwide where the peak *P-T* conditions of UHT metamorphism have been quantified (Jiao *et. al.*, 2023). Ultrahigh Temperature metamorphism named by Harley, 1998 and many researchers suggested that UHT

* Wai Yan Lai Aung, Department of Geology, University of Yangon

metamorphism is a continuum of granulite-facies metamorphism rather than a thermal anomaly (Brown, 2007a, b). The study of microfabric in deformed granulite rocks permits to modeling of some of the complexities of natural tectonic situations (Schmid and Hsü, 1982). In the research, the microfabrics and deformation textures found in granulite are evaluated in the high-temperature/ ultrahigh-temperature metamorphism of the Mogok area in Myanmar. The present research mainly aims to deal with the study of granulite microfabrics and the deformation mechanism significantly found in MMB.

Geologic Setting

Myanmar can be sub-divided into six N–S trending major tectonic domains from west to east: (1) the Arakan (Rakhine) Coastal Strip is an ensimatic fore-deep, (2) the Indo-Burman Ranges represent an outer-arc or fore-arc, (3) the Western Inner-Burman Tertiary Basin is considered to be an inter-arc basin, (4) the Central Volcanic Belt (Central Volcanic Line) represents an inner magmatic-volcanic arc, (5) the Eastern Inner-Burman Tertiary Basin formed as a back-arc basin and (6) the Shan-Tenasserim Massif occurs as ensialic, Sino-Burman Ranges. The Sagaing Fault forms a tectonically significant boundary between the Eastern Inner-Burman Tertiary Basin (back-arc basin) and the continental, ensialic Sino-Burman Ranges (Bender 1983; Khin Zaw *et. al.*, 1989, 1990, 2014) (Figure. 1).

The Mogok area consists of a series of undifferentiated high-grade metamorphic rocks. The dominant unit is banded gneiss, with biotite, garnet, sillimanite, and oligoclase. It is interspersed with quartzite and bands and lenses of marble (Khin Zaw, 1990, 1998; Kyaw Thu, 2007; Themelis, 2008). Wai Yan Lai Aung, 2016, 2017 introduced granulites in Mogok and Momeik areas as felsic and mafic granulites with geological maps (Figure. 2), which are intruded by granitic and syenitic rocks, respectively. The two granulites are generally NE-SW trend with west dipping.

2. Materials and Methods

In this study, methods of the investigations were fixed in detail based on literature reviews, field study, petrological microscopes and advanced techniques such as EDXRF, WDXRF, RAMAN and EPMA analyses. RAMAN and EPMA analysis and imaging were used to determine the mineral composition of assemblages from felsic and mafic granulites. XRFs analysis is used for the bulk rock composition of the granulites. Petrological microscope performed for interpretation of the textures and deformation evidences of mineral grains in the rock, and mineralogical composition of the rock.

3. Result and Discussion

In this paper, the main characteristics of UHT metamorphism are summarized and these provide constraints on the possible physiochemical mechanisms of UHT metamorphism.

3.1 Mineral Assemblage and Texture Evidence for UHT Metamorphism

UHT granulites have typical mineral assemblages of spinel-sillimanite-garnet-orthopyroxene (Li *et. al.*, 2014; Tong *et. al.*, 2013; Yang and Li, 2013; Wang *et. al.*, 2009). UHT metamorphism is primarily recognized based on mineral assemblages found in Mg-Al-rich metapelites (Kelsey and Hand, 2015). The first UHT mineral assemblage recognized from metapelites is sapphirine+quartz (Bhadra, 2016; Tsunogae and Santosh, 2011; Kelsey, 2008), Al-orthopyroxene+sillimanite±quartz, osumilite (Harley, 2008), orthopyroxene+corundum (Kelly and Harley, 2004; Bertrand *et al.*, 1992; Kihle and Bucher-Nurminen, 1992), garnet+corundum (Kelsey *et al.*, 2006; Shimpo *et al.*, 2006; Scrimgeour *et al.*, 2005) and so on. Moreover, some researchers approved the diagnostic minerals and assemblages of UHT metamorphism in Table 1.

Some key mineral assemblages and texture indicators of UHT metamorphism in the Mogok area are described as sapphirine+sillimanite+orthopyroxene+quartz, and perthite+ pyroxene, detailed in (Figure. 3). Distinctive microstructures in granulites and granulitic rocks are highlighted by the representative higher pressure-temperature status, for example, nematoblastic sillimanite layer (Figure. 3a), triple junction of granoblastic polygonal texture (Figure. 3b), helicitic texture of spiral-shaped sillimanite inclusions in garnet porphyroblast (Figure. 3c), kinking biotite layer (Figure. 3c), corona texture and reaction rim of pyroxene minerals (Figure. 3d), replacement texture and some alterations (Figure. 3e) and Symplicitic intergrowth (Figure. 3f, g),

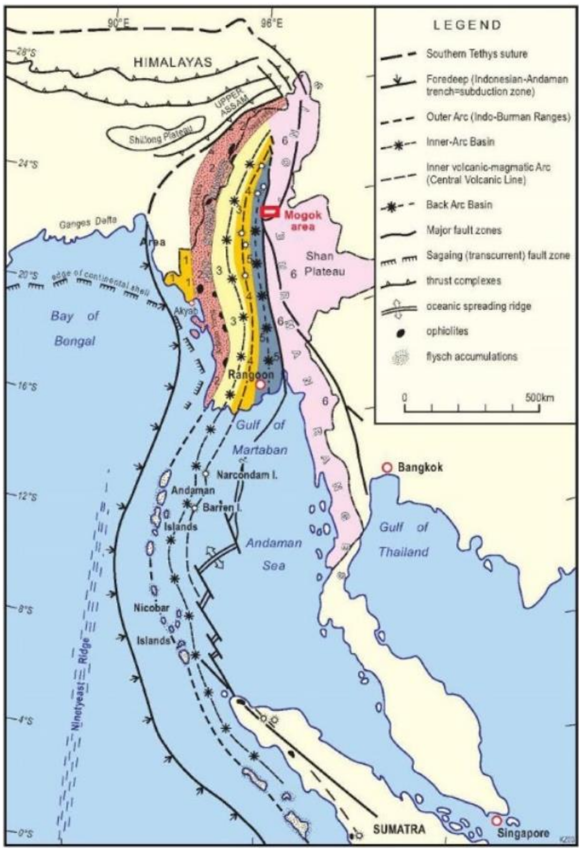

Figure 1. Location map and regional tectonic setting of Mogok area, Myanmar (Bender 1983, Khin Zaw 2014). (1) The Arakan (Rakhine) Coastal Strip, (2) The Indo-Burma Ranges, (3) The Western Inner-Burman Tertiary Basin, (4) The Central Volcanic Belt (Central Volcanic Line), (5) The Eastern Inner-Burman Tertiary Basin, and (6) the Shan-Tenasserim Massif.

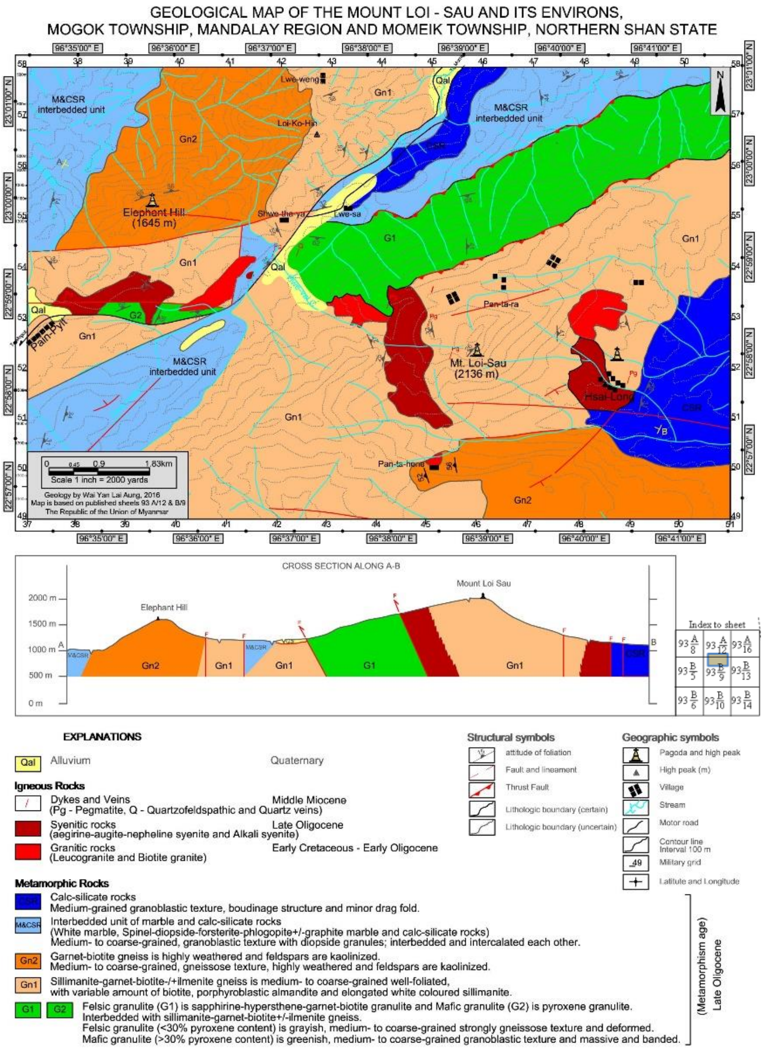

Figure 2. Geological ma p of the boundary area between Mogok and Momeik. Green colour is felsic granulite (G1) and mafic granulite (G2), generally NE-SW trends. (Modified after Wai Yan Lai Aung, 2016, 2018)

3.2 Possible Physiochemical Mechanism

Distinct microstructures in UHT granulites record two endmember types of post-peak metamorphic evolution, which are cooling-dominated (isobaric cooling or IBC) and decompression-dominated (isothermal decompression or ITD) (Jiao *et. al.*, 2023). Some sapphirine-bearing assemblages as coronas around garnet, orthopyroxene or sillimanite are also indicative of UHT metamorphism (Sajeev *et al.*, 2004; Harley, 1998c).

UHT localities with post-peak cooling-dominated paths: Its paths generally record a pressure drop of < 2 kbar, implying limited exhumation after the UHT peak (Jiao *et. al.*, 2023). Microstructures developed during high-temperature cooling include the reactions of sapphirine+quartz to orthopyroxene+sillimanite (Figure 3d) and spinel+quartz to garnet+sillimanite (Figure 3f) and characteristic symplectite of cordierite + orthopyroxene + K-feldspar (Harley, 2nd edt; Korhonen *et. al.*, 2013; Holder *et. al.*, 2018).

UHT localities with post-peak decompression-dominated paths: Its paths generally record a pressure drop of > 2 kbar, although the associated decrease in temperature is variable, implying distinct exhumation mechanisms following the UHT peak (Jiao, 2023). In the Mogok granulites, symplectitic mineral assemblages that replace peak minerals during decompression, such as sapphirine or spinel and cordierite replacing sillimanite, and sapphirine and orthopyroxene replacing garnet (Figure 3g).

Table 1. The diagnostic minerals and assemblages of UHT metamorphism (Jiao, 2023)

Lithology	Minerals and assemblages	References
Metapelites	Sapphirine+quartz	Bhadra (2016); Tsunogae and Santosh (2011); Kelsey (2008); Harley et al. (1990); Ellis (1980)
	Al-orthopyroxene+sillimanite±quartz	Kelsey et al. (2003a, b); White et al. (2001); Carrington and Harley (1995)
	Osumilite and its assemblages	Kelsey and Hand (2015); Sajeev and Osanai (2004); Grew (1982); Ellis (1980)
	Spinel+quartz	Ganguly et al. (2018); Ishii et al. (2006); Dasgupta et al. (1995)
	Al-orthopyroxene+garnet	Ishii et al. (2006); Brandt et al. (2003); Pattison et al. (2003); Harley (1998c)
Mafic granulites	Orthopyroxene+plagioclase± amphibole±ilmenite±spinel	Groppo et al. (2007); Haissen et al. (2004); Nakano et al. (2004); Zhao et al. (2000)
Calc-silicate and carbonate rocks	Clinopyroxene+wollastonite+ scapolite±grossular garnet	Dasgupta and Pal (2005); Sengupta and Raith (2002); Fitzsimons and Harley (1994)
Other minerals and assemblages	Metamorphic pyroxenes	Harley (1987); Sandiford and Powell (1986); Barnicoat and O'Hara (1979)
	Mesoperthite and antiperthite	Lei et al. (2014); Hokada and Suzuki (2006); Prakash et al. (2006); Hokada (2001); Rötzler and Romer (2001)
	Corundum and assemblages	Nicoli et al. (2014); Perchuk et al. (1989); Ellis (1980)

Equilibrated mineral assemblages at UHT peak

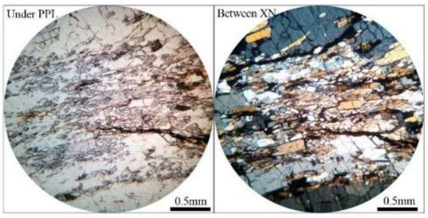

orthopyroxene+sillimanite+sapphirine +quartz in felsic granulite

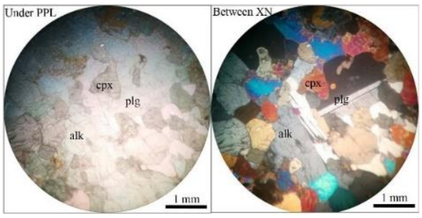

coexistence of perthite and pyroxene in mafic granulite

3a. UHT mineral assemblages in granulites

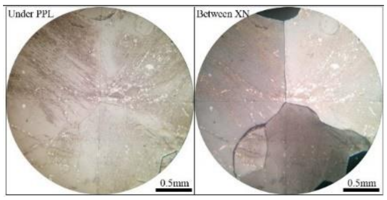

alkali eldspar in granulitic gneiss

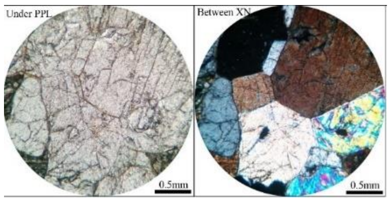

diopside in mafic granulite

3b. Triple junction of granoblastic polygonal textures

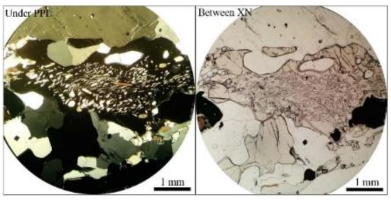

helicitic texture of spiral-shaped sillimanite inclusions in a garnet porphyroblast

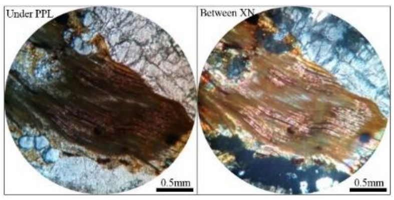

kinking biotite

3c. Distinctive mineral textures in felsic granulites

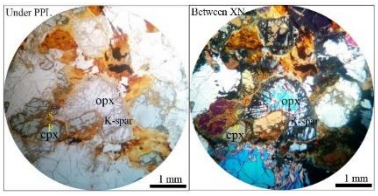

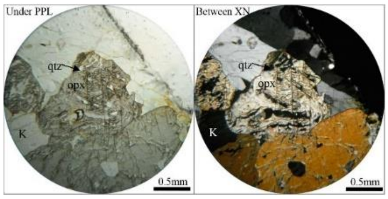

3d. Corona texture and reaction rim of pyroxene in mafic granulites

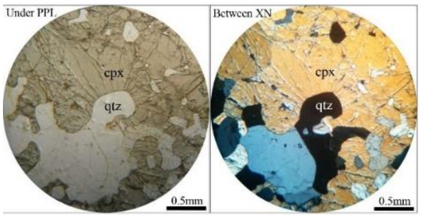

corroded texture

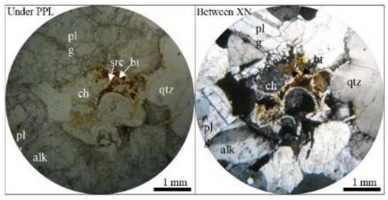

silicification and saussuritization

3e. Replacement textures in mafic granulites

Post-peak cooling-dominated

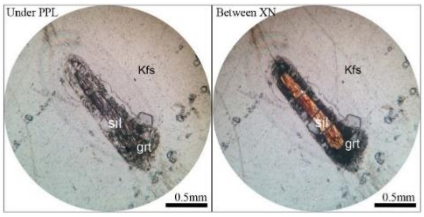

corona texture of sillimanite

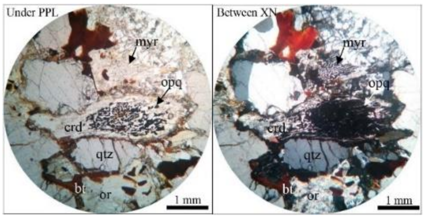

reaction rim of ilmenite

3f. Post-peak cooling dominated replacement textures in felsic granulites

Post-peak decompression-dominated

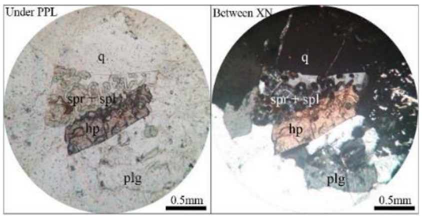

sapphirine, spinel, and cordierite replacing orthopyroxene

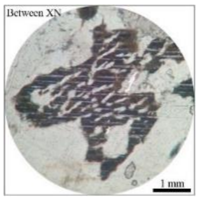

sapphirine and orthopyroxene replacing garnet

3g. Symplicitic intergrowth in felsic granulites

Figure 3, a-g. Some key mineral assemblages and textural indicators of UHT metamorphism

3.3 Geochemistry of Granulites

The UHT metamorphic peak was generally identified in the literature by UHT metamorphism diagnostic equilibrium mineral assemblages, such as sapphirine + quartz + orthopyroxene and orthopyroxene + sillimanite + quartz identified by polarizing microscope (Figure. 3), RAMAN (Figure 4) EPMA (Table 2), and XRF (Figure 5). According to the bulk rock analysis data, felsic granulite has a higher potassium percentage while mafic granulite yields higher calcium content.

Raman analysis on mafic granulite

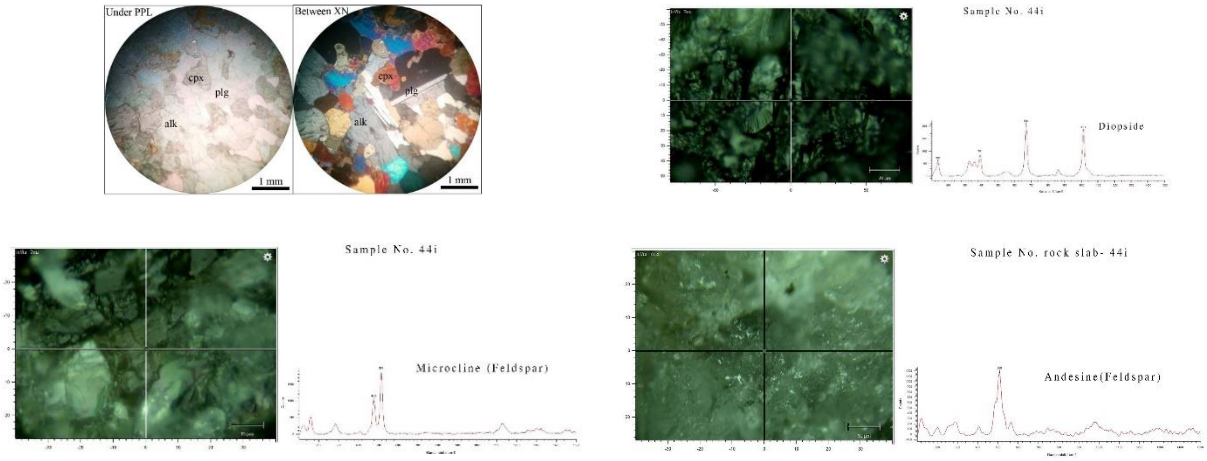

Figure 4. Mineral assemblages of clinopyroxene (diopside), plagioclase (andesine) and microcline in mafic granulite with Raman probe descriptions of selective minerals

EPMA analysis on felsic granulite

Table 2. Mineral chemistry of electron probe microanalysis on felsic granulite

CAS-EPMA 4-2, 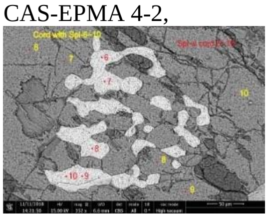	**Si**	53.9	55.	55.8	49.9	50.9	55.7							
	Al	40.4	42.1	42.9	33.9	36.1	43.9							
	Mg	3.1			9.4	7.3								
	Fe	2.3	0.7		6.7	5.7								
	Na	0.4	0.5	0.4			0.4							
	In		0.8	0.9										
Cordierite with spinel	**Ca**		0.4											
CAS-EPMA 9-1, 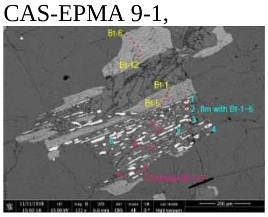	**Si**	40.1	40.0	0.7	50.0	56.1	93.0	100	38.4	37.7	50.3		1	
	Al	18.3	19.4		33.1	29.9			17.5	16.9	34.8			
	Fe	14.6	14.3	45.1	7.4	5.9	7.0		16.0	16.9	6.5	46.3	44.7	45.9
	Mg	11.8	11.6	0.9	9.6	8.1			11.8	11.5	8.5		1.3	
	K	8.8	8.1						8.7	9.1				
	Ti	6.4	6.0	53.2					7.7	8.0		52.4	53.0	54.1
	Na		0.6											
Ilmenite with biotite	**V**											1.3		
CAS-EPMA 11-1, 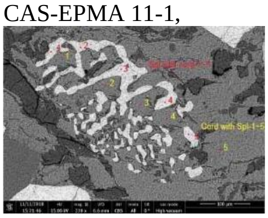	**Al**	60.9	55.9	55.1	60.3	42.3	42.7	33.5	33.4	33.7	43.4	43.2	21.9	31.4
	Fe	27.7	34.4	35.2	28.7	1	1.4	8.8	8.7	5.8			33.8	14.8
	Zn	6.2	4.9	5.0	6.2									
	Mg	5.1	4.8	4.7	4.9			8.0	8.7	7.7			5.1	7.4
	Si					56.4	55.9	49.7	49.1	52.9	55.9	55.9	37.9	46.4
	Na					0.4					0.7	0.9		
Cordierite with spinel	**Ca**												1.3	
CAS-EPMA 19, 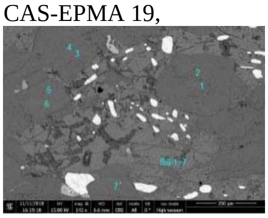	**Si**	54.7	54.2	0.5	1.1	51.0	38.6	38.5	39.1	38.1	37.5			
	Al	41.6	32.6		57.3	31.8	61.4	61.5	60.9	61.9	62.5			
	S	2.2	-											
	Fe	1.0	3.1	45.4	23.4	7.1								
	Na	0.6	0.6											
	K	-	6.0											
	Mg	-	2.8	0.9	5.2	8.9								
	Ti			51.7										
	V			1.5	1.0									
Sillimanite	**Zn**				9.5									
	Cr				1.9									
	P				0.5							21.9		
	Ca	-	-			1.1						33.8		

CAS-EPM 26 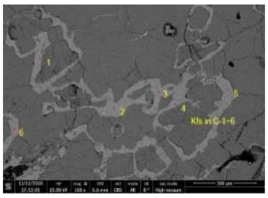 Feldspar	**Si**	65.1	65.4	65.2	37.8	100	36.5
	Al	19.2	18.9	19.5	62.2		63.5
	K	13.5	14.1	13.6	-		
	Na	2.1	16	1.8			

Bulk rock analysis on felsic and mafic granulites

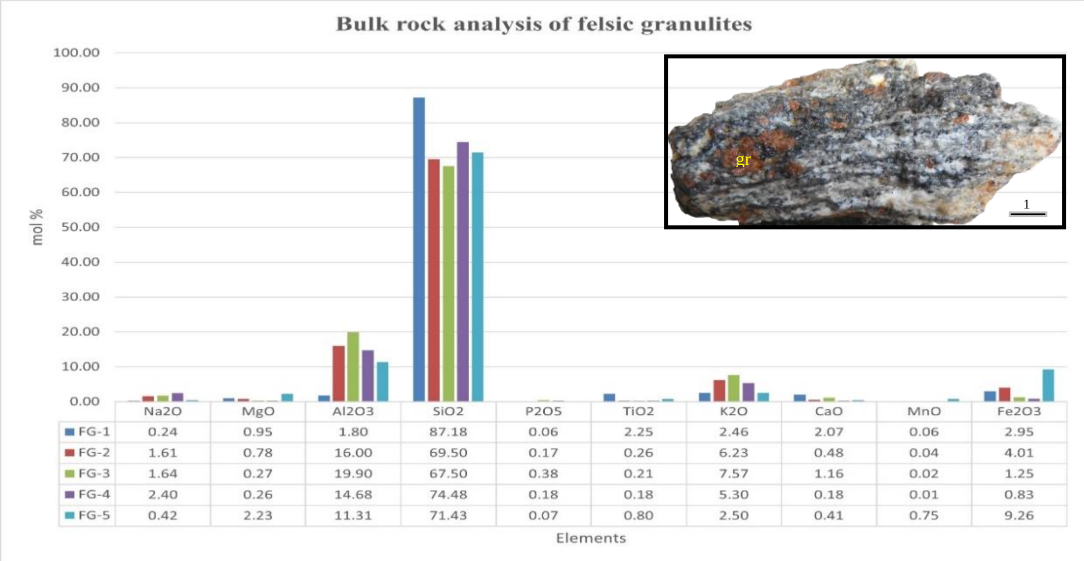

	Na2O	MgO	Al2O3	SiO2	P2O5	TiO2	K2O	CaO	MnO	Fe2O3
FG-1	0.24	0.95	1.80	87.18	0.06	2.25	2.46	2.07	0.06	2.95
FG-2	1.61	0.78	16.00	69.50	0.17	0.26	6.23	0.48	0.04	4.01
FG-3	1.64	0.27	19.90	67.50	0.38	0.21	7.57	1.16	0.02	1.25
FG-4	2.40	0.26	14.68	74.48	0.18	0.18	5.30	0.18	0.01	0.83
FG-5	0.42	2.23	11.31	71.43	0.07	0.80	2.50	0.41	0.75	9.26

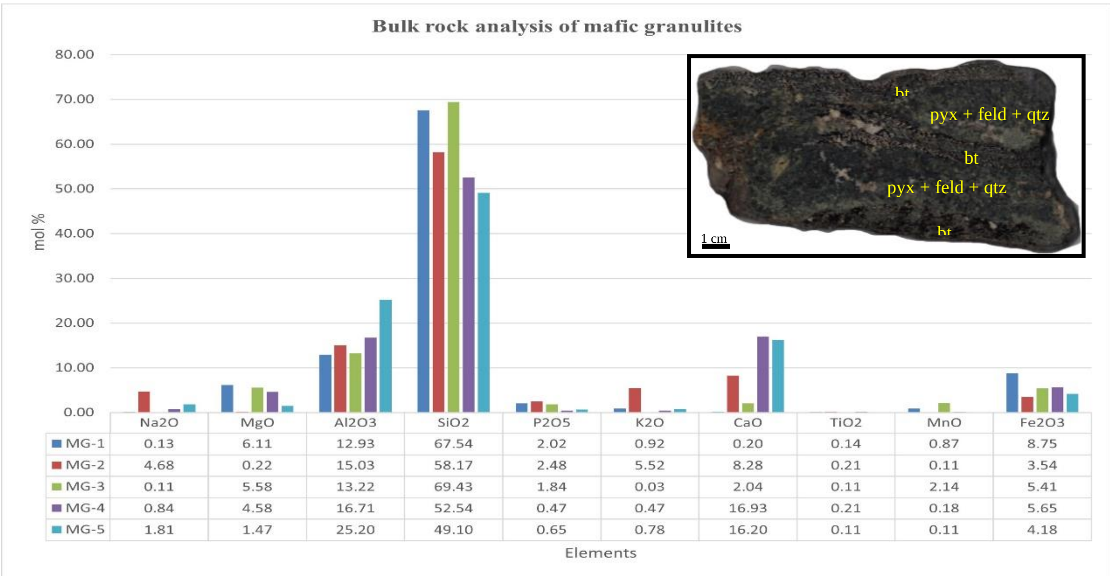

	Na2O	MgO	Al2O3	SiO2	P2O5	K2O	CaO	TiO2	MnO	Fe2O3
MG-1	0.13	6.11	12.93	67.54	2.02	0.92	0.20	0.14	0.87	8.75
MG-2	4.68	0.22	15.03	58.17	2.48	5.52	8.28	0.21	0.11	3.54
MG-3	0.11	5.58	13.22	69.43	1.84	0.03	2.04	0.11	2.14	5.41
MG-4	0.84	4.58	16.71	52.54	0.47	0.47	16.93	0.21	0.18	5.65
MG-5	1.81	1.47	25.20	49.10	0.65	0.78	16.20	0.11	0.11	4.18

Figure 5. Bulk rock analytical data of felsic and mafic granulite

4. Conclusion

Two types of granulites; felsic and mafic are noticeably exposed in the Mogok area and different microstructures in UHT granulites record two endmember types of post-peak metamorphic evolution, which are cooling-dominated (isobaric cooling or IBC) and decompression-dominated (isothermal decompression or ITD) that express retrograde metamorphic *P-T* conditions estimated within the range of 6.5 ~ 7.2 kbar, 700 ~ 780°C.

Acknowledgment

We would like to express our gratitude for financial support from the Asia Research Centre, University of Yangon, Myanmar.

References

Bender, 1983. Geology of Burma.

Bertrand, P., Ouzegane, K., Kienast, J. R., 1992. *P-T-X* Relationships in the Precambrian Al-Mg-Rich Granulites from in Ouzzal, Hoggar, Algeria. *Journal of Metamorphic Geology*, 10(1): 17–31.

Bhadra, S., 2016. Timing and Duration of Ultra-High Temperature Metamorphism in Sapphirine-Bearing Metapelite Granulite from Kodaikanal, Madurai Block, South India: Constraints from Mineral Chemistry and U-Th-Total Pb EPMA Age of Monazite. *Journal of Applied Geochemistry*, 18(1): 22

Brown, M., 2007. Metamorphic conditions in orogenic belts: a record of secular change. *International Geology Review*, *49*(3), pp.193-234.

Chhibber, H.L. 1934a. The Geology of Burma. MacMillan and Co., London.

Chhibber, H.L. 1934b. The Mineral Resources of Burma. MacMillan and Co., London.

Eskola, P., 1952. On the granulites of Lapland. *Am. J. Sci*, *355*, pp.133-171.

Fyfe, W.S., Turner, F.J. and Verhoogen, J., 1961. Coupled reactions in metamorphism: A correction. *Geological Society of America Bulletin*, *72*(1), pp.169-170.

Harley, S. L., 2008. Refining the *P-T* Records of UHT Crustal Metamorphism. *Journal of Metamorphic Geology*, 26(2): 125–154.

Harley, S. L., 1998. *Geology Society Special Publications* Vol. 138 (eds Treloar, P. J. & O'Brien, P. J.) 81–107 (Geological Society of London, 1998).

Holder, R. M., et al., 2018. Ultrahigh-temperature osumilite gneisses in southern Madagascar record combined heat advection and high rates of radiogenic heat production in a long-lived high-*T* orogen. *J. Metamorph. Geol.* **36**, 855–880.

Hughes RW, 1997. Ruby and sapphires. KWH, Boulder

Iyer LAN, 1953. Geology and gemstones of the Mogok stone tract, Burma. Geol Surv India Mem 82:129

Jiao, S., Brown, M., Mitchell, R.N., Chowdhury, P., et. al., 2023. Mechanisms to generate ultrahigh-temperature metamorphism. *Nature Reviews Earth & Environment*, *4*(5), pp.298-318.

Kelly, N. M., Harley, S. L., 2004. Orthopyroxene-Corundum in Mg-Al-Rich Granulites from the Oygarden Islands, East Antarctica. *Journal of Petrology*, 45(7): 1481–1512.

Kelsey, D. E., Clark, C., Hand, M., et al., 2006. Comment on "First Report of Garnet-Corundum Rocks from Southern India: Implications for Prograde High-Pressure (Eclogite-Facies?) Metamorphism". *Earth and Planetary Science Letters*, 249(3/4): 529–534. https://doi.org/10.1016/j.epsl.2006.07.048

Kelsey, D. E., 2008. On Ultrahigh-Temperature Crustal Metamorphism. *Gondwana Research*, 13(1): 1–29. https://doi.org/10.1016/j.gr.2007.06.001

Kelsey, D. E., Hand, M., 2015. On Ultrahigh Temperature Crustal Metamorphism: Phase Equilibria, Trace Element Thermometry, Bulk Composition, Heat Sources, Timescales and Tectonic Settings. *Geoscience Frontiers*, 6(3): 311–356.

Khin Zaw, 1998. Geological evolution of selected granitic pegmatites in Myanmar (Burma): constraints from regional setting, lithology, and fluid-inclusion studies. *International Geology Review*, *40*(7), pp.647-662.

Khin Zaw, Meffre, S., Lai, C.K., et. al., 2014. Tectonics and metallogeny of mainland Southeast Asia—A review and contribution. *Gondwana Research, 26*(1), pp.5-30.

Kihle, J., Bucher-Nurminen, K., 1992. Orthopyroxene-Sillimanite- Sapphirine Granulites from the Bamble Granulite Terrane, Southern Norway. *Journal of Metamorphic Geology*, 10(5): 671–693.

Korhonen, F. J., et al, 2013. Osumilite-melt interactions in ultrahigh temperature granulites: phase equilibria modelling and implications for the *P–T–t* evolution of the Eastern Ghats Province, India. *J. Metamorph. Geol.* 31, 881–907.

Kyaw Thu, 2007. The igneous rocks of the Mogok Stone Tract: their distribution, petrography, petrochemistry, sequence, geochronology and economic geology. *Yangon University, Yangon*.

La Touche, T.D.H, 1913. Geology of the Northern Shan States. Mem- oir of the Geological Survey of India, 39, 33–44.

Lei, H. and Xu, H., 2018. A review of ultrahigh temperature metamorphism. *Journal of Earth Science*, *29*(5), pp.1167-1180.

Li, Z. L., Yang, X. Q., Li, Y. Q., et al., 2014. Late Paleozoic Tectono-Metamorphic Evolution of the Altai Segment of the Central Asian Orogenic Belt: Constraints from Metamorphic *P-T* Pseudosection and Zircon U-Pb Dating of Ultra-High-Temperature Granulite. *Lithos*, 204: 83–96.

Myanmar Geosciences Society, 2014. Geological Map of Myanmar.

Sajeev, K., et al., 2004. Ultrahigh-temperature metamorphism followed by two-stage decompression of garnet-orthopyroxene-sillimanite granulites from Ganguvarpatti, Madurai Block, southern India. *Contrib. Minerol. Petrol.* 148, 29–46.

Schmid, S.M. and Hsü, K.J., 1982. Microfabric studies as indicators of deformation mechanisms and flow laws operative in mountain building. *a= a*, *6*, p.4.

Scrimgeour, I. R., Kinny, P. D., Close, D. F., et al., 2005. High-*T* Granulites and Polymetamorphism in the Southern Arunta Region, Central Australia: Evidence for a 1.64 Ga Accretional Event. *Precambrian Research*, 142(1/2): 1–27.

Searle, D.L. & Haq, B.T, 1964. The Mogok belt of Burma and its relationship to the Himalayan orogeny. Proceedings of the International Geological Congress, 22, 132–161.

Searle, M.P., et al., 2007. Tectonic evolution of the Mogok metamorphic belt, Burma (Myanmar) constrained by U–Th–Pb dating of metamorphic and magmatic rocks. Tectonics, 26, TC3014.

Searle, M. P., et al., 2017. Ch.12. Tectonic and metamorphic evolution of the Mogok Metamorphic and Jade Mines belts and ophiolite terranes of Burma (Myanmar). In A. J. Barber, K. Zaw, & M. J. Crow (Eds.), Myanmar: Geology, Resources and Tectonics, Memoir, (Vol. 48, pp. 261–293). London: Geological Society of London.

Searle, M.P., et al., 2020. Timing of syenite-charnockite magmatism and ruby and sapphire metamorphism in the Mogok Valley Region, Myanmar. *Tectonics*, *39*(3), p.e2019TC005998.

Shimpo, M., Tsunogae, T., Santosh, M., 2006. First Report of Garnet-Corundum Rocks from

Southern India: Implications for Prograde High-Pressure (Eclogite-Facies?) Metamorphism. *Earth and Planetary Science Letters*, 242(1/2): 111–129.

Themelis T, 2008. Gems & mines of Mogok. A & T, Bangkok

Tong, L. X., Chen, Y. B., Xu, Y. G., et al., 2013. Zircon U-Pb Ages of the Ultrahigh-Temperature Metapelitic Granulite from the Altai Orogen, NW China, and Geological Implications. *Acta Petrologica Sinica*, 29(10): 3435–3445

Tsunogae, T., Santosh, M., 2011. Sapphirine+Quartz Assemblage from the Southern Granulite Terrane, India: Diagnostic Evidence for Ultrahigh-Temperature Metamorphism within the Gondwana Collisional Orogen. *Geological Journal*, 46(2/3): 183–197.

Wai Yan Lai Aung, 2016. *Mineralogy and Petrology of the Igneous and Metamorphic Rocks of the Mount Loi-Sau and Its Environs, Momeik Township, Shan State (North)* (Doctoral dissertation, Ph. D, Thesis).

Wai Yan Lai Aung, 2017. Petrology, Phase Equilibria Modelling and P-T Conditions of High-Grade Gneiss from the Mount Loi-Sau and its Environs, Mogok Township, Mandalay Region and Momeik Township, Shan State (North), Journal of the MAAS, Myanmar, Vo.XV, No.5, pp.97-113.

Wai Yan Lai Aung, 2018. Granulite and its P-T Condition of the Mount Loi-Sau and its Environs, Mogok Township, Mandalay Region and Momeik Township, Shan State (North), Journal of the MAAS, Myanmar, Vo.XVI, No.5, pp.131-150.

Wang, W., Wei, C. J., Wang, T., et al., 2009. Confirmation of Pelitic Granulite in the Altai Orogen and Its Geological Significance. *Chinese Science Bulletin*, 54(14): 2543–2548. https://doi.org/10. 1007/s 11434-009-0041-6

Winkler, H.G. and Winkler, H.G., 1965. The Temperature and Pressure Conditions of the Regional Dynamothermal Metamorphism. *Petrogenesis of Metamorphic Rocks*, pp.154-175.

Yang, X. Q., Li, Z. L., 2013. Fluid Characteristics of Late Paleozoic Ultrahigh-Temperature Granulites from the Altay Orogenic Belt, Northwestern China and Its Significance. *Acta Petrologica Sinica*, 29(10): 3446–3456.